

# Buckling and free vibration analysis of tapered FG- CNTRC micro Reddy beam under longitudinal magnetic field using FEM

M. Mohammadimehr\* and S. Alimirzaei

Department of Solid Mechanics, Faculty of Mechanical Engineering, University of Kashan, P.O. Box: 87317-53153, Kashan, Iran

(Received May 10, 2016, Revised December 8, 2016, Accepted December 15, 2016)

**Abstract.** In this paper, the buckling, and free vibration analysis of tapered functionally graded carbon nanotube reinforced composite (FG-CNTRC) micro Reddy beam under longitudinal magnetic field using finite element method (FEM) is investigated. It is noted that the material properties of matrix is considered as Poly methyl methacrylate (PMMA). Using Hamilton's principle, the governing equations of motion are derived by applying a modified strain gradient theory and the rule of mixture approach for micro-composite beam. Micro-composite beam are subjected to longitudinal magnetic field. Then, using the FEM, the critical buckling load, and natural frequency of micro-composite Reddy beam is solved. Also, the influences of various parameters including  $\alpha$  and  $\beta$  (the constant coefficients to control the thickness), three material length scale parameters, aspect ratio, different boundary conditions, and various distributions of CNT such as uniform distribution (UD), unsymmetrical functionally graded distribution of CNT (USFG) and symmetrically linear distribution of CNT (SFG) on the critical buckling load and non-dimensional natural frequency are obtained. It can be seen that the non-dimensional natural frequency and critical buckling load decreases with increasing of  $\beta$  for UD, USFG and SFG micro-composite beam and vice versa for  $\alpha$ . Also, it is shown that at the specified value of  $\alpha$  and  $\beta$ , the dimensionless natural frequency and critical buckling load for SGT beam is more than for the other state. Moreover, it can be observed from the results that employing magnetic field in longitudinal direction of the micro-composite beam increases the natural frequency and critical buckling load. On the other hands, by increasing the imposed magnetic field significantly increases the stability of the system that can behave as an actuator.

**Keywords:** buckling, and free vibration analysis; FG-CNTRC micro-composite Reddy beam; various distribution patterns of CNTs; Strain gradient theory; longitudinal magnetic field; FEM

## 1. Introduction

In recent years, a large amount of literature has been carried out to explore properties and behaviour of micro-composite materials. Functionally graded carbon nanotube reinforced composite (FG-CNTRC) materials are a new breed of micro-composite materials with properties that vary spatially according to a certain non-uniform distribution of the reinforcement phase. Since the carbon nanotube is used as reinforcement in the composite, thus many researchers interested to investigate about this field. They have excellent characteristics such as high aspect ratio, low density, high strength and stiffness. These materials are used widely in various industries including aerospace, automobiles, electronics, optics, chemistry, biomedical engineering, nuclear engineering and mechanical engineering.

Uniform and tapered beams have a wide range of applications from giant structures such as spacecraft's, ships and submarines, micro- and nano-electro-mechanical system (MEMS and NEMS) devices, including biomedical applications, micro-sensors and micro-actuators.

So many researches in the field of static, buckling, and

vibration analysis are done by researchers on them (Lau *et al.* 2004). To verify the performance of the numerical methods, numerical results of them are compared with those of the existing displacement based finite element models (Reddy 2004, 1987). For each beam bending model, three types of boundary conditions (clamped-clamped (CC), hinged-hinged (HH), and pinned-pinned (PP) boundary conditions) are examined and the results are compared with the other results. Vibrations of non-uniform functionally graded (FG) multi-walled carbon nanotubes (MWCNTs) - polystyrene nano-composite beams under action of moving load are presented by Heshmati and Yas (2013). Their results illustrated that the symmetrical linear distribution of MWCNTs results with an increase in the fundamental natural frequency of nano-composite beams which are higher than those of beams with uniform and unsymmetrical MWCNTs distributions. In the other work, dynamic analysis of functionally graded multi-walled carbon nanotube-polystyrene nano-composite beams subjected to multi-moving loads is studied by Heshmati and Yas (2013). Sahmani and Ansari (2013) illustrated size-dependent buckling analysis of functionally graded third-order shear deformable micro-beams including thermal environment effect. They obtained that temperature change plays more important role in the buckling behavior of FG micro-beams with higher values of dimensionless length scale parameter. Zhang and co-workers (2014) studied non-classical Timoshenko beam element based on the strain gradient

---

\*Corresponding author,  
E-mail: mmohammadimehr@kashanu.ac.ir

theory (SGT). Their numerical results showed that small size effects are significant when the thickness of beam is small, but become negligible with increasing thickness of beam. Also, some results can be employed as a benchmark for further studies. Free vibration and buckling analysis of Timoshenko beams reinforced by single-walled carbon nanotubes (SWCNTs) is considered by Yas and Samadi (2012). Their results illustrated that several parameters such as various boundary conditions, the value of volume fraction of CNTs and the stiffness of elastic foundation are effective in free vibration and buckling characteristics of beam. Static and nonlinear vibration analysis of micro beams based on elastic foundation using Euler-Bernoulli beam theory is investigated by Simsek (2014). They considered the effects of the length scale parameter and the stiffness coefficients of the nonlinear foundation on the static deflection and the ratio of nonlinear frequency to linear frequency. Mohammadimehr and Rahmati (2013) presented the electro-thermo-mechanical nonlocal axial vibration analysis of single-walled boron-nitride nano-rods (SWBNRs) under electric excitation. They obtained the constitutive equation for the nano-rods under electro-thermo-mechanical loadings, then they discussed about effects of the aspect ratio, small scale parameter, clamped-clamped and clamped-free boundary conditions on the natural frequency. Strain gradient beam elements are illustrated by Kahrobaiyan and co-workers (2014). Their results observed that there is a good agreement between the experimental and the strain gradient based FEM results while the difference between the experimental and the classical FEM results is significant. In addition, it is indicated that the new beam element can successfully capture the size dependency and the structures modelled by this element show stiffer behavior than those modelled by the classical beam element. Ghiasian *et al.* (2014) studied non-linear rapid heating of FG beams. Ghorbanpour Arani *et al.* (2016) presented modelling and vibration control of axially moving laminated carbon nanotubes/fiber/polymer composite (CNTFPC) plate under initial tension. They obtained the governing equations of the laminated CNTFPC plates based on first-order shear deformation plate theory (FSDT). They obtained that, thermally induced vibrations indeed exist especially for the case of sufficiently thin beams. Sahmani *et al.* (2015) investigated the free vibration characteristics of post buckled third-order shear deformable functionally graded material (FGM) nano-beams including surface effects. Their obtained results revealed that the natural frequency of FGM nano-beam decreases by increasing the value of material property gradient index. Also, it is revealed that the surface effect plays more important role on the vibration characteristics of the buckled FGM nano-beams with lower thicknesses. Large-amplitude free vibrations of FG beams by means of a finite element formulation are studied by Hemmatnezhad *et al.* (2013). Their results showed that the power exponent increases, both linear and nonlinear frequencies decrease. This is due to the deviation of the beam from pure alumina to steel as it grows up from zero to infinity. Zhang *et al.* (2016) investigated a two-level method for static and dynamic analysis of multi-layered composite beam and

plate. Their obtained results indicated that the Misses stress contours and the maximum stress of the coarse element with the global-local higher-order theory are quite coincident with the traditional FEM. Ghorbanpour and co-workers (2012) presented nonlinear vibration of SWBNNTs based on nonlocal Timoshenko beam theory using differential quadrature method (DQM). They concluded that imposing a direct electric potential in axially polarized direction causes decreasing fundamental frequency and applying it in reverse direction increases it. Vibration analysis of non-uniform and non-homogeneous boron nitride nanorods embedded in an elastic medium under combined loadings using DQM is studied by Rahmati and Mohammadimehr (2014). It is concluded that frequency ratio decreases considering electrothermal loadings are more effective in non-uniform nanorods, in comparison with uniform nanorod. Also, the natural frequency of boron nitride nanotube (BNNRs) can be varied using different cross section coefficient and non-homogeneity parameter. Mohammadimehr *et al.* (2016) investigated size dependent effect on the buckling and vibration analysis of double-bonded nanocomposite piezoelectric plate reinforced by BNNT based on modified couple stress theory (MCST). The results of their research showed that the critical buckling load decreases with an increase in the dimensionless material length scale parameter. Thermal postbuckling behavior of size-dependent FG Timoshenko microbeams is taken into account by Ansari *et al.* (2013). Their numerical results presented with an increase in the values of material gradient index and dimensionless length scale parameter leads to larger thermal postbuckling deflections. Dynamic analysis of FG nano-composite beams reinforced by randomly oriented CNT under the action of moving load is studied by Yas and Heshmati (2012). Their obtained results indicated that a CNT-reinforced composite can possibly reach superior vibrational properties only if the CNTs are controlled to be aligned in the whole material. Chakraborty *et al.* (2002) investigated finite element analysis of free vibration and wave propagation in asymmetric composite beam with structural discontinuities. Their results from the analysis showed that the formulated element predicts response that compares very well with the available results. Taati and co-workers (2014) investigated size-dependent generalized thermo elasticity model for Timoshenko micro-beams based on strain gradient and non-Fourier heat conduction theories. They compared the results for two cases including the modified couple stress and the classical continuum theories. The illustration of the existence of thermal damping in the coupled thermo elastic problem is another important contribution of their study. Mohammadimehr *et al.* (2015) investigated the free vibration of viscoelastic double-bonded polymeric nanocomposite plates reinforced by FG-SWCNTs using modified strain gradient theory (MSGT), sinusoidal shear deformation theory and meshless method. Their results showed that the elastic foundation, vdW interaction and magnetic field increase the dimensionless natural frequency of the double-bonded nano-composite plates for CT, MCST and MSGT. Also the material length scale parameter effects on the non-dimensional natural frequency of the double

bonded nano-composite plates are negligible at  $h/l \geq 5$  for CT, and MCST and MSGT. Karimov *et al.* (2014) presented temperature gradient sensor based on CNT composite. They studied the thin film temperature gradient sensor using the composite of CNT and polymer adhesive. A new beam finite element for the analysis of functionally graded materials is studied by Chakraborty *et al.* (2003). Their results demonstrated that the static model is an effective way to smoothen stress jumps in bi-material beams. Ishaquddin *et al.* (2016) investigated efficient coupled polynomial interpolation scheme for out-of-plane free vibration analysis of curved beams. The results showed that the stiffness and consistent mass matrices generated from the coupled displacement models excellent convergence of natural frequencies. Giannopoulos *et al.* (2014) presented mechanical properties of graphene based nano-composites incorporating a hybrid interphase. Their numerical results showed that the linear enhancement of the reinforced component is observed as volume fraction increases.

In this paper, the buckling, and free vibration analysis of tapered FG-CNTRC micro beam using FEM is investigated for various distributions of CNTs and different boundary conditions. Based on the Hamilton's principle type, the governing equations of equilibrium are obtained. Also the influences of various parameters including  $\alpha$  and  $\beta$ , three material length scale parameters, aspect ratio, different boundary conditions, and various distributions of CNT such as UD, USFG and SFG on the critical buckling load and non-dimensional natural frequency are illustrated.

## 2. Material Properties of CNTRC Beams

According to Fig. 1, the tapered micro-composite beam is considered with length  $L$  and thickness  $h(x)$  (Mohammadimehr *et al.* 2015). This micro-composite beam rested on Pasternak elastic foundation. The Pasternak foundation is described by a two-parameter model that the first parameter  $k_w$  is the spring constant of the usual Winkler foundation and the second parameter  $k_g$  represents the shear constant of Pasternak foundation.

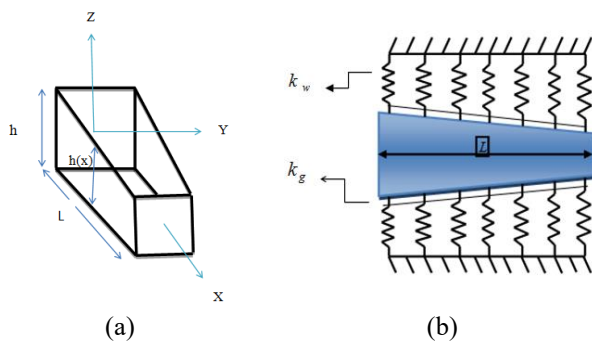


Fig. 1 An schematic view of geometry and coordinate system for tapered micro-composite beam rested on Pasternak foundation

The rule of mixture is employed to estimate the effective properties of carbon nanotube reinforced composites (CNTRC) material. For FG micro-composite beam reinforced by SWCNT, one can be written the following equation (Yas and Samadi 2012, Shen 2009)

$$V_{CNT} + V_m = 1 \quad (1)$$

where  $V_{CNT}$  and  $V_m$  are CNT and matrix volume fractions, respectively.  $V_{CNT}$  is defined for different distribution of CNT. In this paper, three types of CNT distribution are assumed as follows (Yas and Samadi 2012, Shen 2009)

Uniform distribution (UD)

$$V_{CNT} = \bar{V}_{CNT} \quad (2)$$

Unsymmetrical functionally graded distribution of CNT (USFG)

$$V_{CNT}(z) = \left(1 - \frac{2z}{h}\right) \bar{V}_{CNT} \quad (3)$$

Symmetrically linear distribution of CNT (SFG)

$$V_{CNT}(z) = 2 \left(\frac{2|z|}{h}\right) \bar{V}_{CNT} \quad (4)$$

where  $h$  is the thickness of micro-composite beam at  $x=0$  and  $V_{CNT}$  is considered as the following form (Heshmati and Yas 2013)

$$\bar{V}_{CNT} = \frac{W_{CNT}}{W_{CNT} + \left(\frac{\rho_{CNT}}{\rho_m}\right) - \left(\frac{\rho_{CNT}}{\rho_m}\right)W_{CNT}} \quad (5)$$

$W_{CNT}$ ,  $\rho_{CNT}$  and  $\rho_m$  are mass fraction of CNT, density of CNT and matrix, respectively.

According to rule of mixture model, the effective Young's modulus, shear modulus, Poisson's ratio and mass density of CNTRC Reddy beams can be expressed as (Yas and Samadi 2012, Shen 2009)

$$\begin{aligned} E_{11} &= \eta_1 V_{CNT} E_{11}^{CNT} + V_m E_m \\ \frac{\eta_2}{E_{22}} &= \frac{V_{CNT}}{E_{22}^{CNT}} + \frac{V_m}{E_m} \\ \frac{\eta_3}{G_{12}} &= \frac{V_{CNT}}{G_{12}^{CNT}} + \frac{V_m}{G_m} \\ \nu_{12} &= V_{CNT} \nu_{CNT} + V_m \nu_m \\ \rho &= V_{CNT} \rho_{CNT} + V_m \rho_m \end{aligned} \quad (6)$$

where,  $E_{11}^{CNT}$ ,  $E_{22}^{CNT}$ ,  $G_{12}^{CNT}$ ,  $\nu_{CNT}$ ,  $\rho_{CNT}$  and  $E_m$ ,  $G_m$ ,  $\nu_m$ ,  $\rho_m$  indicate the Young's modulus, shear modulus, Poisson's ratios and density of CNT and matrix, respectively.  $\eta_i$  ( $i=1,2,3$ ) denotes the size dependent material properties.

Also thermal expansion coefficient is expressed as follows (Shen 2009)

$$\alpha = V_{CNT} \alpha_{11}^{CNT} + V_m \alpha_m \quad (7)$$

where,  $\alpha_{11}^{CNT}$  and  $\alpha_m$ , are thermal expansion coefficients of CNT and matrix, respectively that are obtained by the following form (Shen 2009)

$$\begin{aligned}\alpha_{CNT} &= 1.0777 \times 10^{-8} \times (T - 300) + 3.4584 \\ \alpha_m &= 4.5 \times 10^{-5} \times (1 + 0.0005(T - 300))\end{aligned}\quad (8)$$

### 3. Theory and formulations

#### 3.1 Maxwell's relations

The governing electrostatics Maxwell equations are written as follows (Narendar *et al.* 2012)

$$\begin{aligned}h = \text{Curl}(\mathbf{U} \times \mathbf{H}) &= \nabla \times \begin{vmatrix} u & 0 & w \\ H_x & 0 & 0 \end{vmatrix} = \nabla \times (0, wH_x, 0) = \begin{vmatrix} \frac{\partial}{\partial x} & \frac{\partial}{\partial y} & \frac{\partial}{\partial z} \\ 0 & wH_x & 0 \end{vmatrix} \\ (-\frac{\partial}{\partial z}wH_x, 0, \frac{\partial}{\partial x}wH_x) &= (0, 0, \frac{\partial}{\partial x}wH_x) \\ \mathbf{f} = \mu \times (\mathbf{J} \times \mathbf{h}) &= \mu \times \begin{vmatrix} 0 & -\frac{\partial}{\partial x}(\frac{\partial}{\partial x}wH_x) & 0 \\ H_x & 0 & 0 \end{vmatrix} = \mu H_x^2 \frac{\partial}{\partial x}(\frac{\partial w}{\partial x}) = \mu H_x^2 \frac{\partial^2 w}{\partial x^2}\end{aligned}\quad (9)$$

where  $\mathbf{H} = (H_x, 0, 0)$  is magnetic field vector and  $\mu$  is the magnetic field permeability.

Therefore the component of Lorentz forces along the  $x$ ,  $y$  and  $z$  directions states as follows

$$f_x = 0, f_y = 0, f_z = \mu H_x^2 \left( \frac{\partial^2 w}{\partial x^2} \right) \quad (10)$$

#### 3.2 The virtual form of motion equations for FG-CNTRC micro-composite Reddy beam

The displacement fields for FG-CNTRC micro-composite beam are derived based on third-order shear deformation theory at any point of the beam can be written as (Sahmani *et al.* 2013, Sahmani and Ansari 2015):

$$\begin{aligned}u_1(x, z, t) &= u(x, t) + z\psi(x, t) - \frac{4z^3}{3h^2}(\psi(x, t) + \frac{\partial w}{\partial x}), \quad \bar{c} = \frac{4}{3h^2} \\ u_3(x, z, t) &= w(x, t), \quad u_2(x, z, t) = 0\end{aligned}\quad (11)$$

In which the displacement fields  $u_1$ ,  $u_2$  and  $u_3$  represent components of displacement vector in  $x$ ,  $y$  and  $z$  directions, respectively, and  $u$  and  $w$  denote the displacements on the mid-plane along  $x$  and  $z$  directions, respectively.

Assuming small deformations, the strains in terms of displacements can be written as

$$\begin{cases} \varepsilon_{ij} = \frac{1}{2}(u_{i,j} + u_{j,i}) \\ \varepsilon_{xx} = \frac{\partial u}{\partial x} + z \frac{\partial \psi}{\partial x} - \frac{4z^3}{3h^2} \left( \frac{\partial \psi}{\partial x} + \frac{\partial^2 w}{\partial x^2} \right) \\ \varepsilon_{xz} = \frac{1}{2} \left( \frac{\partial w}{\partial x} + \psi \right) - \frac{2z^2}{h^2} \left( \psi + \frac{\partial w}{\partial x} \right) \end{cases} \quad (12)$$

Based on the SGT, the dilatation gradient,  $\gamma_i$ , deviatoric stretch gradient,  $\eta_{ijk}^{(1)}$ , and symmetric rotation gradient

tensors,  $\chi_{ij}$ , are defined as (Lam *et al.* 2003)

$$\begin{aligned}\gamma_i &= \varepsilon_{mm,i} \\ \eta_{ijk}^{(1)} &= \frac{1}{3}(\varepsilon_{jk,i} + \varepsilon_{ki,j} + \varepsilon_{ij,k}) - \frac{1}{15}(\varepsilon_{mm,k} + 2\varepsilon_{mk,m}) - \\ &\quad \frac{1}{15}[\delta_{jk}(\varepsilon_{mm,i} + 2\varepsilon_{mi,m}) + \delta_{ki}(\varepsilon_{mm,j} + 2\varepsilon_{mj,m})] \\ \chi_{ij} &= \frac{1}{2} \left( \frac{\partial \theta_i}{\partial x_j} + \frac{\partial \theta_j}{\partial x_i} \right), \quad i, j = 1, 2, 3\end{aligned}\quad (13)$$

where  $\theta_i$  is the components of the rotation vector that can be expressed as follows

$$\theta_i = \frac{1}{2}(\text{curl}(\mathbf{u}))_i \quad (14)$$

also

$$\theta_1 = \frac{1}{2} \left( \frac{\partial u_3}{\partial x_2} - \frac{\partial u_2}{\partial x_3} \right), \quad \theta_2 = \frac{1}{2} \left( \frac{\partial u_1}{\partial x_3} - \frac{\partial u_3}{\partial x_1} \right), \quad \theta_3 = \frac{1}{2} \left( \frac{\partial u_2}{\partial x_1} - \frac{\partial u_1}{\partial x_2} \right) \quad (15)$$

Substituting Eqs. (11) and (12) into Eq. (13) yields the following form

$$\begin{aligned}\theta_2 &= \frac{1}{2} \left( \psi - \frac{\partial w}{\partial x} \right) - \frac{2z^2}{h^2} \left( \psi + \frac{\partial w}{\partial x} \right) \\ \chi_{xy} = \chi_{yx} &= \frac{1}{4} \left( \frac{\partial \psi}{\partial x} - \frac{\partial^2 w}{\partial x^2} \right) - \frac{z^2}{h^2} \left( \frac{\partial \psi}{\partial x} + \frac{\partial^2 w}{\partial x^2} \right) \\ \chi_{yz} = \chi_{zy} &= -\frac{2z}{h^2} \left( \psi + \frac{\partial w}{\partial x} \right) \\ \gamma_{xxx} &= \frac{\partial \varepsilon_{xx}}{\partial x} = \frac{\partial^2 u}{\partial x^2} + z \frac{\partial^2 \psi}{\partial x^2} - \frac{4z^3}{3h^2} \left( \frac{\partial^2 \psi}{\partial x^2} + \frac{\partial^3 w}{\partial x^3} \right) - \alpha_x \Delta T_x \\ \gamma_{xxx} &= \frac{\partial \varepsilon_{xx}}{\partial z} = \frac{\partial \psi}{\partial x} - \frac{12z^2}{3h^2} \left( \frac{\partial \psi}{\partial x} + \frac{\partial^2 w}{\partial x^2} \right) - (\alpha_x \Delta T)_z \\ \eta_{xxx} &= \frac{2}{5} \left( \frac{\partial^2 u}{\partial x^2} + z \frac{\partial^2 \psi}{\partial x^2} \right) - \frac{8z^3}{15h^2} \left( \frac{\partial^2 \psi}{\partial x^2} + \frac{\partial^3 w}{\partial x^3} \right) + \frac{8z}{5h^2} \left( \psi + \frac{\partial w}{\partial x} \right) - \frac{2}{5} (\alpha_x \Delta T)_x \\ \eta_{xxx} &= -\frac{1}{5} \left( \frac{\partial^2 \psi}{\partial x^2} + 2 \frac{\partial \psi}{\partial x} \right) + \frac{8z^2}{5h^2} \left( \frac{\partial \psi}{\partial x} + \frac{\partial^2 w}{\partial x^2} \right) + \frac{1}{5} (\alpha_x \Delta T)_z \\ \eta_{xxx} &= \eta_{xxx} = \eta_{xxx} = \frac{4}{15} \left( \frac{\partial^2 \psi}{\partial x^2} + 2 \frac{\partial \psi}{\partial x} \right) - \frac{32z^2}{15h^2} \left( \frac{\partial \psi}{\partial x} + \frac{\partial^2 w}{\partial x^2} \right) - \frac{4}{15} (\alpha_x \Delta T)_x \\ \eta_{yyy} &= \eta_{yyy} = \eta_{yyy} = -\frac{1}{5} \left( \frac{\partial^2 u}{\partial x^2} + z \frac{\partial^2 \psi}{\partial x^2} \right) + \frac{4z^3}{15h^2} \left( \frac{\partial^2 \psi}{\partial x^2} + \frac{\partial^3 w}{\partial x^3} \right) + \frac{8z}{15h^2} \left( \psi + \frac{\partial w}{\partial x} \right) + \frac{1}{5} (\alpha_x \Delta T)_x \\ \eta_{yyy} &= \eta_{yyy} = \eta_{yyy} = -\frac{1}{15} \left( \frac{\partial^2 \psi}{\partial x^2} + 2 \frac{\partial \psi}{\partial x} \right) + \frac{8z^2}{15h^2} \left( \frac{\partial \psi}{\partial x} + \frac{\partial^2 w}{\partial x^2} \right) + \frac{1}{15} (\alpha_x \Delta T)_z \\ \eta_{xxx} &= \eta_{xxx} = \eta_{xxx} = -\frac{1}{5} \left( \frac{\partial^2 u}{\partial x^2} + z \frac{\partial^2 \psi}{\partial x^2} \right) - \frac{32z^2}{15h^2} \left( \frac{\partial \psi}{\partial x} + \frac{\partial^2 w}{\partial x^2} \right) + \frac{4z^3}{15h^2} \left( \frac{\partial^2 \psi}{\partial x^2} + \frac{\partial^3 w}{\partial x^3} \right) + \frac{1}{5} (\alpha_x \Delta T)_x\end{aligned}\quad (16)$$

Furthermore, for a linear orthotropic elastic material, the corresponding higher order stress can be obtained by the following constitutive relations:

$$\begin{Bmatrix} \sigma_x \\ \sigma_y \\ \sigma_z \\ \sigma_{yz} \\ \sigma_{xz} \\ \sigma_{xy} \end{Bmatrix} = \begin{bmatrix} c_{11} & c_{12} & c_{13} & 0 & 0 & 0 \\ c_{21} & c_{22} & c_{23} & 0 & 0 & 0 \\ c_{31} & c_{32} & c_{33} & 0 & 0 & 0 \\ 0 & 0 & 0 & c_{44} & 0 & 0 \\ 0 & 0 & 0 & 0 & c_{55} & 0 \\ 0 & 0 & 0 & 0 & 0 & c_{66} \end{bmatrix} \begin{Bmatrix} \varepsilon_x \\ \varepsilon_y \\ \varepsilon_z \\ 2\varepsilon_{yz} \\ 2\varepsilon_{xz} \\ 2\varepsilon_{xy} \end{Bmatrix} - \begin{Bmatrix} \alpha_x \\ 0 \\ 0 \\ 0 \\ 0 \\ 0 \end{Bmatrix} \Delta T \quad (17)$$

$$p_i = 2\mu l_0^2 \gamma_i$$

$$\tau_{ijk}^{(1)} = 2\mu l_1^2 \eta_{ijk}^{(1)}$$

$$m_{ij} = 2\mu l_2^2 \chi_{ij}$$

where  $l_0$ ,  $l_1$  and  $l_2$  are three material length scale parameters denote the dilatation gradients, deviatoric stretch gradients and rotation gradients, respectively. Also  $c_{ij}$  and  $\mu$  denote components of elastic stiffness coefficient and shear modulus, respectively.

Moreover, the parameters  $p_i$ ,  $\tau_{ijk}^{(1)}$ , and  $m_{ij}$  represent the higher-order stresses; also  $\sigma_{ij}$  and  $\varepsilon_{ij}$  are normal stress and strain, respectively.

The strain, kinetic energy, the virtual work done by the external forces and the work done by the axial force  $P_M$  of the FG micro-composite beam reinforced by CNTs are written as follows

$$T = \frac{1}{2} \int_0^L \rho(z) (\dot{U}^2 + \dot{W}^2 + \dot{\psi}^2) dA dx$$

$$S = \frac{1}{2} \int_0^L \int_0^A \left( \sigma_{xx} \varepsilon_{xx} + \tau_{xz} \gamma_{xz} + P_{xxx} Y_{xxx} + P_{xxx} Y_{xxx} + 2m_{xy} \chi_{xy} + 2m_{yz} \chi_{yz} + \tau_{xxx} \eta_{xxx} + \tau_{zzz} \eta_{zzz} + 3\tau_{xxz} \eta_{xxz} + 3\tau_{xyy} \eta_{xyy} + 3\tau_{xzz} \eta_{xzz} + 3\tau_{yyz} \eta_{yyz} \right) dA dx \quad (18)$$

$$R = b \int_0^L (-k_w w + k_s \frac{\partial^2 w}{\partial x^2}) W dx$$

$$\gamma_p = -\frac{1}{2} \int_0^L P_M \left( \frac{\partial w}{\partial x} \right)^2 dA$$

Finally, Lorentz work is written as

$$\Omega_{Lorentz} = \int f_z \delta w dA \quad (19)$$

where

$$\sigma_x = c_{11} (\varepsilon_x - \alpha_x \Delta T)$$

$$\gamma_{xz} = c_{55} \left( 1 - \frac{4z^2}{h^2} \right) (\psi + \frac{\partial w}{\partial x})$$

$$P_{xxx} = 2G_{12} l_0^2 Y_{xxx}, \quad P_{xxz} = 2G_{12} l_0^2 Y_{xxz}$$

$$m_{xy} = 2G_{12} l_2^2 \chi_{xy}, \quad m_{yz} = 2G_{12} l_2^2 \chi_{yz} \quad (20)$$

$$\tau_{xxx} = 2G_{12} l_1^2 \eta_{xxx}, \quad \tau_{zzz} = 2G_{12} l_1^2 \eta_{zzz}$$

$$\tau_{xxz} = 2G_{12} l_1^2 \eta_{xxz}, \quad \tau_{xyy} = 2G_{12} l_1^2 \eta_{xyy}$$

$$\tau_{xzz} = 2G_{12} l_1^2 \eta_{xzz}, \quad \tau_{yyz} = 2G_{12} l_1^2 \eta_{yyz}$$

where  $c_{11}$  and  $c_{55}$  are elastic stiffness coefficients which are defined as

$$c_{11} = \frac{E_{11}}{1 - \nu_{12}^2}, \quad c_{55} = G_{12} \quad (21)$$

According to Hamilton's principle, the variation form of the motion equation can be considered as:

$$\delta \Pi = \delta S - (\delta T + \delta R + \delta \gamma_p + \delta \Omega_{Lorentz}) = 0 \quad (22)$$

According to the strain gradient theory, the variation form of strain energy and virtual work done by the external forces are expressed as follows (Reddy 2004)

$$\delta S = \frac{1}{2} \int_0^L \int_0^A \left( \delta \sigma_{xx} \varepsilon_{xx} + \delta \tau_{xz} \gamma_{xz} + \delta P_{xxx} Y_{xxx} + \delta P_{xxx} Y_{xxx} + 2\delta m_{xy} \chi_{xy} + 2\delta m_{yz} \chi_{yz} + \delta \tau_{xxx} \eta_{xxx} + \delta \tau_{zzz} \eta_{zzz} + 3\delta \tau_{xxz} \eta_{xxz} + 3\delta \tau_{xyy} \eta_{xyy} + 3\delta \tau_{xzz} \eta_{xzz} + 3\delta \tau_{yyz} \eta_{yyz} \right) dA dx \quad (23)$$

$$\delta R = \int \delta w \left( -k_w w + k_s \frac{\partial^2 w}{\partial x^2} \right) dA$$

$$\delta \gamma_p = \int \delta w \left( \frac{\partial w}{\partial x} \right)^2 dA$$

$$\delta \Omega_{Lorentz} = \int f_z \delta w dA$$

### 3.3 Finite Element Method (FEM)

In this paper, FEM is used to solve the governing equations of FG-CNTRC micro-composite Reddy beams. According to FEM, the axial displacement  $u$ , transverse deflection  $w$  and rotation  $\psi_x$  are interpolated as follows (Reddy 2004)

$$u(x) = N_1 u_1 + N_2 w_1 + N_3 \psi_1 + N_4 u_2 + N_5 w_2 + N_6 \psi_2 = [N_u(x)] \{q_u\}$$

$$w(x) = N_7 w_1 + N_8 \psi_1 + N_9 w_2 + N_{10} \psi_2 = [N_w(x)] \{q_w\} \quad (24)$$

$$\psi_x(x) = N_{11} w_1 + N_{12} \psi_1 + N_{13} w_2 + N_{14} \psi_2 = [N_\psi(x)] \{q_\psi\}$$

where  $N_i$  ( $i=1, \dots, 14$ ) are the associated shape functions for axial, transverse and rotational degrees of freedom, respectively, that step calculation of expression as follows:

The interpolation functions of displacement fields for the finite-element formulation are considered as follows (Heshmati and Yas 2013, Chakraborty *et al.* 2002)

$$u(x) = c_1 + c_2 x + c_3 x^2$$

$$w(x) = c_4 + c_5 x + c_6 x^2 + c_7 x^3 \quad (25)$$

$$\psi_x(x) = c_8 + c_9 x + c_{10} x^2$$

Eq. (25) has ten constants and only six boundary conditions (three degrees of freedom at each node of the element). The four additional dependent constants can be expressed in terms of six other independent constants by substituting Eq. (25) into the governing equations of motion, so we have

$$c_7 = -\frac{1}{3} c_{10}, \quad c_6 = -\frac{1}{2} c_9, \quad c_3 = -\frac{A_1}{A_0} c_{10}$$

$$c_8 = \left( \frac{-8A_0 A_1 h^2 - 6A_1^2 h^4 + 8A_0 A_2 h^2 + 6A_0 A_3 h^4}{A_0(3B_0 h^4 - 16B_1 h^2 + 16B_2)} \right) c_{10} + \left( \frac{-3A_0 B_0 h^4 + 16A_0 B_1 h^2 - 16A_0 B_2}{A_0(3B_0 h^4 - 16B_1 h^2 + 16B_2)} \right) c_5 \quad (26)$$

By substituting Eq. (26) into Eq. (25), the displacement fields are derived as the following form

$$u = c_1 + c_2 x + \left( -\frac{A_1}{A_0} c_{10} \right) x^2$$

$$w = c_4 + c_5 x + \left( -\frac{1}{2} c_9 \right) x^2 + \left( -\frac{1}{3} c_{10} \right) x^3 \quad (27)$$

$$\psi_x = \left( \frac{-8A_0 A_1 h^2 - 6A_1^2 h^4 + 8A_0 A_2 h^2 + 6A_0 A_3 h^4}{A_0(3B_0 h^4 - 16B_1 h^2 + 16B_2)} + x^2 \right) c_{10} + \left( \frac{-3A_0 B_0 h^4 + 16A_0 B_1 h^2 - 16A_0 B_2}{A_0(3B_0 h^4 - 16B_1 h^2 + 16B_2)} \right) c_5 + c_9 x$$

The equations of FEM displacements for an element of FG-CNTRC micro-composite Reddy beam can be expressed as follows (Heshmati and Yas 2013, Chakraborty *et al.* 2002)

$$[q] = \begin{bmatrix} u \\ w \\ \psi_x \end{bmatrix} = \begin{bmatrix} 1 & x & 0 & 0 & 0 & \left( -\frac{A_1}{A_0} \right) x^2 \\ 0 & 0 & 1 & x & -\frac{x^2}{2} & -\frac{x^3}{3} \\ 0 & 0 & 0 & \left( \frac{-8A_0 A_1 h^2 - 6A_1^2 h^4 + 8A_0 A_2 h^2 + 6A_0 A_3 h^4}{A_0(3B_0 h^4 - 16B_1 h^2 + 16B_2)} + x^2 \right) & \left( \frac{-3A_0 B_0 h^4 + 16A_0 B_1 h^2 - 16A_0 B_2}{A_0(3B_0 h^4 - 16B_1 h^2 + 16B_2)} \right) x & c_9 \end{bmatrix} \begin{bmatrix} c_1 \\ c_2 \\ c_3 \\ c_4 \\ c_5 \\ c_9 \end{bmatrix} \quad (28)$$

$$= [N(x)] \{a\}, \quad \{a\} = [c_1, c_2, c_3, c_4, c_5, c_9]^T$$

where  $[N_i(x)]$  is the matrix containing functions of  $x$  and it is of size  $3 \times 6$ . The column vector  $\{a\}$  of independent constants can be expressed in terms of nodal displacements by substituting six displacement boundary conditions into Eq. (28). For  $x=0$  (node 1) and  $x=l_e$  (node 2) we obtain (Heshmati and Yas 2013, Chakraborty *et al.* 2002)

$$[G]^{-1} = \begin{Bmatrix} N(0) \\ N(l_e) \end{Bmatrix}, \quad \{\hat{q}\} = [G]^{-1} \{a\}, \quad \{a\} = [G] \{\hat{q}\}, \quad l_e = \frac{L}{\text{number of elements}} \quad (29)$$

Finally, we have

$$\{q\} = \begin{Bmatrix} u(x) \\ w(x) \\ \psi_x(x) \end{Bmatrix} = [N(x)]\{a\} = [N(x)][G]\{\hat{q}\} = [\bar{N}(x)]\{\hat{q}\}$$

$$\bar{N}(x) = \begin{bmatrix} N_1 & N_2 & N_3 & N_4 & N_5 & N_6 \\ 0 & N_7 & N_8 & 0 & N_9 & N_{10} \\ 0 & N_{11} & N_{12} & 0 & N_{13} & N_{14} \end{bmatrix} = \begin{bmatrix} N_u(x) \\ N_w(x) \\ N_\psi(x) \end{bmatrix} \quad (30)$$

Finally, the shape functions are obtained as follows

$$\begin{aligned} N_1 &= 1 - \frac{x}{l_e}, & N_2 &= -(6\hat{c}_1)x + \left(\frac{6\hat{c}_1}{l_e}\right)x^2, & N_3 &= (3\hat{c}_1 l_e)x - (3\hat{c}_1)x^2 \\ N_4 &= \frac{x}{l_e}, & N_5 &= (6\hat{c}_1)x - \left(\frac{6\hat{c}_1}{l_e}\right)x^2, & N_6 &= (3\hat{c}_1 l_e)x - (3\hat{c}_1)x^2 \\ N_7 &= 1 - \left(\frac{\hat{c}_2}{l_e}\right)x - (3\hat{c}_3)x^2 + \left(\frac{2\hat{c}_3}{l_e}\right)x^3, & N_8 &= -(\hat{c}_4)x + \left(\frac{\hat{c}_5}{l_e}\right)x^2 - (\hat{c}_3)x^3 \\ N_9 &= \left(\frac{\hat{c}_2}{l_e}\right)x + (3\hat{c}_3)x^2 - \left(\frac{2\hat{c}_3}{l_e}\right)x^3, & N_{10} &= \left(\frac{\hat{c}_2}{2}\right)x + \left(\frac{\hat{c}_6}{l_e}\right)x^2 - (\hat{c}_3)x^3 \\ N_{11} &= (6\hat{c}_7)x - \left(\frac{6\hat{c}_7}{l_e}\right)x^2, & N_{12} &= (3\hat{c}_7)x^2 - \left(\frac{2\hat{c}_5}{l_e}\right)x + 1 \\ N_{13} &= (-6\hat{c}_7)x + \left(\frac{6\hat{c}_7}{l_e}\right)x^2, & N_{14} &= (3\hat{c}_7)x^2 - \left(\frac{2\hat{c}_6}{l_e}\right)x \end{aligned} \quad (31)$$

where

$$A_i = b \int_{\frac{he'}{2}}^{\frac{he'}{2}} z^i c_{11} dz, \quad B_i = b \int_{\frac{he'}{2}}^{\frac{he'}{2}} z^i G_{12} dz; \quad i = 0, 1, 2, \dots$$

$$R_1 = (3B_0 h_0^4 - 16B_2 h_0^2 + 16B_4)$$

$$R_2 = (-48A_0 A_4 h_0^2 - 36A_1^2 h_0^4 + 48A_1 A_3 h_0^2 + 36A_0 A_2 h_0^4)$$

$$\hat{c}_1 = \frac{A_0 R_1}{[(A_0 l_e^2)R_1 + R_2]}, \quad \hat{c}_2 = \frac{R_2}{[(A_0 l_e^2)R_1 + R_2]}, \quad \hat{c}_3 = \frac{A_0 A_1 R_1}{[(A_0 l_e^2)R_1 + R_2]} \quad (32)$$

$$\hat{c}_4 = \frac{(A_0 l_e^2)R_1 + \frac{R_2}{2}}{[(A_0 l_e^2)R_1 + R_2]}, \quad \hat{c}_5 = \frac{(4A_0 l_e^2)R_1 + R_2}{2[(A_0 l_e^2)R_1 + R_2]}, \quad \hat{c}_6 = \frac{(2A_0 l_e^2)R_1 - R_2}{2[(A_0 l_e^2)R_1 + R_2]}$$

$$\hat{c}_7 = \frac{A_0 R_1}{[(A_0 l_e^2)R_1 + R_2]}$$

By substituting Eq. (30) into Eqs. (12) and (16), the components of strain, the dilatation gradients, deviatoric stretch gradients and rotation gradient are shown in Appendix A.

Also by substituting Eq. (24) into Eq. (18) and the variation form of the kinematic energy is written as

$$\delta \mathcal{E} = \int_{\Omega} \int_{\Omega} \rho(z) \left[ \begin{aligned} & \left( \{\delta q_\alpha\}^T [N_\alpha] + z \{\delta q_\alpha\}^T [N_\alpha] - \frac{4z^3}{3h^2} (\{\delta q_\alpha\}^T [N_\alpha] + \{\delta q_\alpha\}^T \frac{d}{dx} [N_\alpha]) \right) \times \\ & \left( [N_\alpha] \{\hat{q}_\alpha\} + z [N_\alpha] \{\hat{q}_\alpha\} - \frac{4z^3}{3h^2} ([N_\alpha] \{\hat{q}_\alpha\} + \frac{d}{dx} [N_\alpha] \{\hat{q}_\alpha\}) \right) + \\ & \left( \{\delta q_\alpha\}^T [N_\alpha] [N_\alpha] \{\hat{q}_\alpha\} \right) \end{aligned} \right] dA dx \quad (33)$$

Substituting Eqs. (23) and (33) into Eq. (22), the equations of motion can be derived as follows

$$\begin{aligned} & \left( \sum_{j=1}^m K_{ij}^{11} u_j + \sum_{j=1}^n K_{ij}^{12} w_j + \sum_{j=1}^p K_{ij}^{13} \psi_j \right) + \left( \sum_{j=1}^m M_{ij}^{11} \ddot{u}_j + \sum_{j=1}^n M_{ij}^{12} \ddot{w}_j + \sum_{j=1}^p M_{ij}^{13} \ddot{\psi}_j \right) = 0 \\ & \left( \sum_{j=1}^m K_{ij}^{21} u_j + \sum_{j=1}^n K_{ij}^{22} w_j + \sum_{j=1}^p K_{ij}^{23} \psi_j \right) + \left( \sum_{j=1}^m M_{ij}^{21} \ddot{u}_j + \sum_{j=1}^n M_{ij}^{22} \ddot{w}_j + \sum_{j=1}^p M_{ij}^{23} \ddot{\psi}_j \right) = 0 \\ & \left( \sum_{j=1}^m K_{ij}^{31} u_j + \sum_{j=1}^n K_{ij}^{32} w_j + \sum_{j=1}^p K_{ij}^{33} \psi_j \right) + \left( \sum_{j=1}^m M_{ij}^{31} \ddot{u}_j + \sum_{j=1}^n M_{ij}^{32} \ddot{w}_j + \sum_{j=1}^p M_{ij}^{33} \ddot{\psi}_j \right) = 0 \end{aligned} \quad (34)$$

where the elements of stiffness and mass matrices are

written as follows

\*Element stiffness matrices

$$\begin{aligned} K_{ij}^{11} &= \int_{x_a}^{x_b} A_1 \frac{d[N_u]^T}{dx} \frac{d[N_u]}{dx} dx + \int_{x_a}^{x_b} \left( 21\frac{l_e^2}{5} + \frac{4}{5} l_e^2 \right) B_0 \frac{d^2[N_u]^T}{dx^2} \frac{d^2[N_u]}{dx^2} dx \\ K_{ij}^{12} &= \int_{x_a}^{x_b} \left( \frac{4}{3h^2} \right) A_3 \frac{d[N_w]^T}{dx} \frac{d^2[N_w]}{dx^2} dx + \int_{x_a}^{x_b} \left( \frac{48}{15} \frac{l_e^2}{h^2} \right) B_1 \frac{d^2[N_w]^T}{dx^2} \frac{d^2[N_w]}{dx^2} dx - \\ & \int_{x_a}^{x_b} \left( \frac{8}{3} \frac{l_e^2}{h^2} + \frac{16}{15} \frac{l_e^2}{h^2} \right) B_3 \frac{d^2[N_w]^T}{dx^2} \frac{d^3[N_w]}{dx^3} dx \\ K_{ij}^{13} &= \int_{x_a}^{x_b} \left( A_1 - \frac{4}{3h^2} A_3 \right) \frac{d[N_\psi]^T}{dx} \frac{d[N_\psi]}{dx} dx + \int_{x_a}^{x_b} \left( \frac{48}{15} \frac{l_e^2}{h^2} \right) B_1 \frac{d^2[N_\psi]^T}{dx^2} [N_\psi] dx + \\ & \int_{x_a}^{x_b} \left( 21\frac{l_e^2}{5} + \frac{4}{5} l_e^2 \right) B_1 - \left( \frac{8}{3} \frac{l_e^2}{h^2} + \frac{16}{15} \frac{l_e^2}{h^2} \right) B_3 \frac{d^2[N_\psi]^T}{dx^2} \frac{d^2[N_\psi]}{dx^2} dx \end{aligned} \quad (35a)$$

$$\begin{aligned} K_{ij}^{21} &= \int_{x_a}^{x_b} \left( \frac{4}{3h^2} \right) A_3 \frac{d^2[N_w]^T}{dx^2} \frac{d[N_w]}{dx} dx + \int_{x_a}^{x_b} \left( \frac{48}{15} \frac{l_e^2}{h^2} \right) B_1 \frac{d[N_w]^T}{dx} \frac{d^2[N_w]}{dx^2} dx - \\ & \int_{x_a}^{x_b} \left( \frac{8}{3} \frac{l_e^2}{h^2} + \frac{16}{15} \frac{l_e^2}{h^2} \right) B_3 \frac{d^3[N_w]^T}{dx^3} \frac{d^2[N_w]}{dx^2} dx \\ K_{ij}^{22} &= \int_{x_a}^{x_b} \left( \frac{32}{9} \frac{l_e^2}{h^2} + \frac{64}{45} \frac{l_e^2}{h^2} \right) B_0 \frac{d^3[N_w]^T}{dx^3} \frac{d^2[N_w]}{dx^2} dx + \\ & \int_{x_a}^{x_b} \left( \frac{16}{9h^2} A_6 + \left( \frac{32}{h^2} l_e^2 + \frac{4l_e^2}{h^2} + \frac{512}{15} \frac{l_e^2}{h^2} \right) B_1 + \left( \frac{64}{15} \frac{l_e^2}{h^2} \right) B_2 \right) \frac{d^2[N_w]^T}{dx^2} \frac{d^2[N_w]}{dx^2} dx + \\ & \int_{x_a}^{x_b} \left( \frac{2l_e^2}{h^2} - \frac{128}{15} \frac{l_e^2}{h^2} \right) B_2 + \left( \frac{1}{4} l_e^2 + \frac{4}{5} l_e^2 \right) B_0 \frac{d^2[N_w]^T}{dx^2} \frac{d^3[N_w]}{dx^3} dx + \\ & \int_{x_a}^{x_b} \left( B_0 - \frac{8}{h^2} B_2 + \frac{16}{h^2} B_4 + \left( \frac{16l_e^2}{h^4} + \frac{512}{15} \frac{l_e^2}{h^4} \right) B_2 \right) \frac{d[N_w]^T}{dx} \frac{d[N_w]}{dx} dx - \\ & \int_{x_a}^{x_b} \left( \frac{64}{15} \frac{l_e^2}{h^2} \right) B_4 \frac{d^3[N_w]^T}{dx^3} \frac{d[N_w]}{dx} dx - \int_{x_a}^{x_b} \left( \frac{64}{15} \frac{l_e^2}{h^2} \right) B_4 \frac{d[N_w]^T}{dx} \frac{d^3[N_w]}{dx^3} dx + \\ & b \int_{x_a}^{x_b} k_\alpha [N_w]^T [N_w] dx - b \int_{x_a}^{x_b} k_\beta [N_w]^T \frac{d^2[N_w]}{dx^2} dx - b \int_{x_a}^{x_b} \mu H z^2 [N_w]^T \frac{d^2[N_w]}{dx^2} dx \\ K_{ij}^{23} &= \int_{x_a}^{x_b} \left( \frac{16}{9h^2} A_6 + \left( \frac{32}{h^2} l_e^2 + \frac{4l_e^2}{h^2} + \frac{512}{15} \frac{l_e^2}{h^2} \right) B_1 - \left( \frac{8l_e^2}{h^2} + \frac{64}{5} \frac{l_e^2}{h^2} \right) B_2 \right) \frac{d^2[N_w]^T}{dx^2} \frac{d[N_\psi]}{dx} dx + \\ & \int_{x_a}^{x_b} \left( -\frac{1}{4} l_e^2 + \frac{16}{15} l_e^2 \right) B_4 - \frac{4}{3h^2} A_4 \frac{d^2[N_w]^T}{dx^2} \frac{d[N_\psi]}{dx} dx + \\ & \int_{x_a}^{x_b} \left( B_0 - \frac{8}{h^2} B_2 + \frac{16}{h^2} B_4 + \left( \frac{16l_e^2}{h^4} + \frac{512}{15} \frac{l_e^2}{h^4} \right) B_2 \right) \frac{d[N_w]^T}{dx} [N_\psi] dx - \\ & \int_{x_a}^{x_b} \left( \frac{32}{9} \frac{l_e^2}{h^2} + \frac{64}{45} \frac{l_e^2}{h^2} \right) B_0 + \left( \frac{8}{3} \frac{l_e^2}{h^2} + \frac{16}{15} \frac{l_e^2}{h^2} \right) B_2 \frac{d^2[N_w]^T}{dx^2} \frac{d^2[N_\psi]}{dx^2} dx - \\ & + \int_{x_a}^{x_b} \left( \frac{64}{15} \frac{l_e^2}{h^2} \right) B_4 \frac{d^3[N_w]^T}{dx^3} [N_\psi] dx + \int_{x_a}^{x_b} \left( \frac{16}{5} \frac{l_e^2}{h^2} \right) B_1 - \left( \frac{64}{15} \frac{l_e^2}{h^2} \right) B_4 \frac{d[N_w]^T}{dx} \frac{d^2[N_\psi]}{dx^2} dx \end{aligned} \quad (35b)$$

$$\begin{aligned} K_{ij}^{31} &= \int_{x_a}^{x_b} \left( A_1 - \frac{4}{3h^2} A_3 \right) \frac{d[N_\psi]^T}{dx} \frac{d[N_\psi]}{dx} dx + \int_{x_a}^{x_b} \left( \frac{48}{15} \frac{l_e^2}{h^2} \right) B_1 [N_\psi]^T \frac{d^2[N_\psi]}{dx^2} dx + \\ & \int_{x_a}^{x_b} \left( 21\frac{l_e^2}{5} + \frac{4}{5} l_e^2 \right) B_1 - \left( \frac{8}{3} \frac{l_e^2}{h^2} + \frac{16}{15} \frac{l_e^2}{h^2} \right) B_3 \frac{d^2[N_\psi]^T}{dx^2} \frac{d^2[N_\psi]}{dx^2} dx \\ K_{ij}^{32} &= \int_{x_a}^{x_b} \left( \frac{16}{9h^2} A_6 + \left( \frac{32}{h^2} l_e^2 + \frac{4l_e^2}{h^2} + \frac{512}{15} \frac{l_e^2}{h^2} \right) B_1 - \left( \frac{8l_e^2}{h^2} + \frac{64}{5} \frac{l_e^2}{h^2} \right) B_2 \right) \frac{d[N_\psi]^T}{dx} \frac{d^2[N_\psi]}{dx^2} dx + \\ & \int_{x_a}^{x_b} \left( -\frac{1}{4} l_e^2 + \frac{16}{15} l_e^2 \right) B_0 - \frac{4}{3h^2} A_4 \frac{d[N_\psi]^T}{dx} \frac{d^2[N_\psi]}{dx^2} dx - \\ & \int_{x_a}^{x_b} \left( B_0 - \frac{8}{h^2} B_2 + \frac{16}{h^2} B_4 + \left( \frac{16l_e^2}{h^4} + \frac{512}{15} \frac{l_e^2}{h^4} \right) B_2 \right) [N_\psi]^T \frac{d[N_\psi]}{dx} dx - \\ & \int_{x_a}^{x_b} \left( \frac{32}{9} \frac{l_e^2}{h^2} + \frac{64}{45} \frac{l_e^2}{h^2} \right) B_0 + \left( \frac{8}{3} \frac{l_e^2}{h^2} + \frac{16}{15} \frac{l_e^2}{h^2} \right) B_2 \frac{d^2[N_\psi]^T}{dx^2} \frac{d^2[N_\psi]}{dx^2} dx - \\ & + \int_{x_a}^{x_b} \left( \frac{64}{15} \frac{l_e^2}{h^2} \right) B_4 [N_\psi]^T \frac{d^2[N_\psi]}{dx^2} dx + \int_{x_a}^{x_b} \left( \frac{16}{5} \frac{l_e^2}{h^2} \right) B_1 - \left( \frac{64}{15} \frac{l_e^2}{h^2} \right) B_4 \frac{d^2[N_\psi]^T}{dx^2} \frac{d[N_\psi]}{dx} dx \\ K_{ij}^{33} &= \int_{x_a}^{x_b} \left( A_2 - \frac{8}{3h^2} A_4 + \frac{16}{9h^2} A_6 \right) + \left( 21\frac{l_e^2}{5} + \frac{4}{5} l_e^2 \right) B_0 - \\ & \int_{x_a}^{x_b} \left( \frac{16}{h^2} l_e^2 + \frac{2l_e^2}{h^2} + \frac{256}{15} \frac{l_e^2}{h^2} \right) B_2 + \left( \frac{32}{h^2} l_e^2 + \frac{4l_e^2}{h^2} + \frac{512}{15} \frac{l_e^2}{h^2} \right) B_4 \frac{d[N_\psi]^T}{dx} \frac{d[N_\psi]}{dx} dx + \\ & \int_{x_a}^{x_b} \left( B_0 - \frac{8}{h^2} B_2 + \frac{16}{h^2} B_4 + \left( \frac{16l_e^2}{h^4} + \frac{512}{15} \frac{l_e^2}{h^4} \right) B_2 \right) [N_\psi]^T [N_\psi] dx + \\ & \int_{x_a}^{x_b} \left( 21\frac{l_e^2}{5} + \frac{4}{5} l_e^2 \right) B_1 - \left( \frac{8}{3} \frac{l_e^2}{h^2} + \frac{16}{15} \frac{l_e^2}{h^2} \right) B_3 + \left( \frac{32}{9} \frac{l_e^2}{h^2} + \frac{64}{45} \frac{l_e^2}{h^2} \right) B_0 \frac{d^2[N_\psi]^T}{dx^2} \frac{d^2[N_\psi]}{dx^2} dx \\ & + \int_{x_a}^{x_b} \left( \frac{16}{5} \frac{l_e^2}{h^2} B_1 - \frac{64}{15} \frac{l_e^2}{h^2} B_3 \right) \frac{d^2[N_\psi]^T}{dx^2} [N_\psi] dx + \int_{x_a}^{x_b} \left( \frac{16}{5} \frac{l_e^2}{h^2} B_1 - \frac{64}{15} \frac{l_e^2}{h^2} B_3 \right) [N_\psi]^T \frac{d^2[N_\psi]}{dx^2} dx \end{aligned} \quad (35c)$$

\*Element mass matrices:

$$\left\{ \begin{aligned} M_{11} &= \int_{x_a}^{x_b} I_0 [N_u]^T [N_u] dx \\ M_{12} &= \frac{-4}{3h^2} \int_{x_a}^{x_b} I_3 [N_u]^T \frac{d[N_w]}{dx} dx \\ M_{13} &= \int_{x_a}^{x_b} \left( I_1 - \frac{4}{3h^2} I_3 \right) [N_u]^T [N_\psi] dx \\ M_{21} &= \frac{-4}{3h^2} \int_{x_a}^{x_b} I_3 \frac{d[N_w]^T}{dx} [N_u] dx \\ M_{22} &= \frac{16}{9h^4} \int_{x_a}^{x_b} I_6 \frac{d[N_w]^T}{dx} \frac{d[N_w]}{dx} dx + \int_{x_a}^{x_b} I_0 [N_w]^T [N_w] dx \\ M_{23} &= \int_{x_a}^{x_b} \left( \frac{16}{9h^4} I_6 - \frac{4}{3h^2} I_4 \right) \frac{d[N_w]^T}{dx} [N_\psi] dx \\ M_{31} &= \int_{x_a}^{x_b} \left( I_1 - \frac{4}{3h^2} I_3 \right) [N_\psi]^T [N_u] dx \\ M_{32} &= \int_{x_a}^{x_b} \left( \frac{16}{9h^4} I_6 - \frac{4}{3h^2} I_4 \right) [N_\psi]^T \frac{d[N_w]}{dx} dx \\ M_{33} &= \int_{x_a}^{x_b} \left( I_2 - \frac{8}{3h^2} I_4 + \frac{16}{9h^4} I_6 \right) [N_\psi]^T [N_\psi] dx \end{aligned} \right. \quad (36)$$

Also, the coefficients of stiffness matrix and mass moment of inertia for each element are considered as

$$A_i = b \int_{-\frac{he^i}{2}}^{\frac{he^i}{2}} z^i c_{11} dz, \quad B_i = b \int_{-\frac{he^i}{2}}^{\frac{he^i}{2}} z^i G(z) dz \quad (37a)$$

$$I_0^i = b \int_{-\frac{he^i}{2}}^{\frac{he^i}{2}} z^i p(z) dz, \quad i = 0, 1, 2, 3, \dots \quad (37b)$$

where  $h_e^i$  is the thickness for each element,  $\alpha$  and  $\beta$  are the constant coefficients to control the thickness variations of FG-CNTRC micro-composite tapered Reddy beam (Heshmati and Yas 2013)

$$h_e^i = \frac{h_0}{l_e^i} \left[ l_e^i - \frac{\beta}{(\alpha + 1)l^\alpha} ((x_z^e)^{\alpha+1} - (x_1^e)^{\alpha+1}) \right] \quad (38)$$

The coefficient of stability matrix can be written as

$$[G] = P_M \int_{x_a}^{x_b} \frac{d[N_w]^T}{dx} \frac{d[N_w]}{dx} dx \quad (39)$$

So the motion equations of FG-CNTRC micro-composite Reddy beam can be obtained as the following matrix form

$$([K] - \omega^2 [M]) \{q\} = 0 \quad (40-a)$$

$$([K] - P_M [G]) \{q\} = 0 \quad (40-b)$$

The element stiffness matrix in Eq. (40) is defined by

sub-matrices  $[k_{ij}^{11}]$ ,  $[k_{ij}^{12}]$ ,  $[k_{ij}^{13}]$  and  $[k_{ij}^{21}]$ ,  $[k_{ij}^{22}]$ ,  $[k_{ij}^{23}]$  and  $[k_{ij}^{31}]$ ,  $[k_{ij}^{32}]$ ,  $[k_{ij}^{33}]$ ; which are defined in Appendix B.

The various boundary conditions of the micro-composite beams such as Simply-Simply (S-S), clamped-clamped (C-C), clamped-free (C-F) are considered that are described as follows

Clamped (C):  $u = w = \frac{dw}{dx} = 0$

Free (F):  $N_x = 0, Q_x = 0$

Simply Support (S):  $u = w = 0, M_x = 0$

#### 4. Numerical results and discussions

In this article, the buckling and free vibration analysis of tapered FG-CNTRC micro Reddy beam based on SGT under longitudinal magnetic field using FEM is investigated. The physical, geometrical and mechanical parameters of FG-CNTRC micro-composite Reddy beam are considered in Table 1.

##### 4.1 Free vibration and buckling analysis of micro-composite reddy beam model

In this part, the effects of the various distributions of CNTs, variation boundary conditions and longitudinal magnetic field changes on non-dimensional natural frequency and critical buckling load are discussed. Also the influence of various  $\beta$  and  $\alpha$  for different dimensionless material length scale parameters on the dimensionless natural frequency and critical buckling load is presented. The dimensionless natural frequency is considered as follows (Yas and Samadi 2012)

$$\Omega = \omega L \sqrt{\frac{I_{10}}{A_{110}}} \quad (41)$$

where  $A_{110}$  and  $I_{10}$  are the values of  $A_1$  and  $I_0$  of a homogeneous beam made of pure matrix material, respectively.

In Table 2, the dimensionless natural frequencies of

Table 1 The geometrical, mechanical and physical parameters of FG-CNTRC micro-composite Reddy beam (Yas and Samadi 2012)

parameter	value	parameter	value	parameter	value
$V_{CNT}$	0.12	$\eta_1$	1.2833	$\eta_2$	1.0556
$P_m$	1900 $\frac{kg}{m^3}$	$P_{CNT}$	1400 $\frac{kg}{m^3}$	$v_m$	0.3
$v_{CNT}$	0.19	$E_{CNT}$	600 GPa	$E_m$	2.5 GPa
$\mu$	$4\pi \times 10^{-7} \frac{H}{m}$	$k_g$	$10^{-5} \frac{N}{m}$	$k_w$	$10^{12} \frac{N}{m^3}$
$b/h_0$	2	$l/h_0$	1	$L/h_0$	10

Table 2 Comparison between the results of present work (FEM) and the obtained results by Yas and Samadi (2012) ( $L/h=15$ )

*	UD		FG-USFG		FG-SFG	
	Present work	Yas and Samadi	Present work	Yas and Samadi	Present work	Yas and Samadi
$V_{CNT}=0.12$	0.37668	0.3764	0.31991	0.3193	0.44158	0.4416
C-F	1.50603	1.5085	1.40609	1.4068	1.59564	1.6000

CNT Timoshenko beam is calculated using present FEM method with various boundary conditions and compared with the obtained results by (Yas and Samadi 2012) for the following mechanical properties

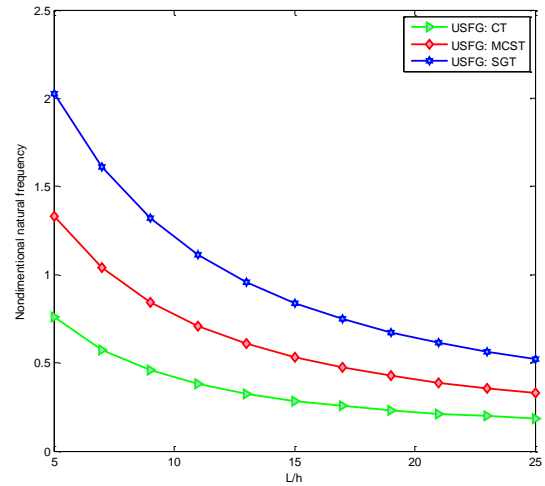
$$E_{11}^{CNT} = 600GPa \quad E_m = 2.5GPa \quad \nu_{CNT} = 0.19 \quad \nu_m = 0.3 \quad G_{12}^{CNT} = 17.2GPa$$

$$\rho_{CNT} = 1400 \frac{kg}{m^3} \quad \rho_m = 1900 \frac{kg}{m^3} \quad k_w = k_s = 0 \quad \bar{c} = 0$$

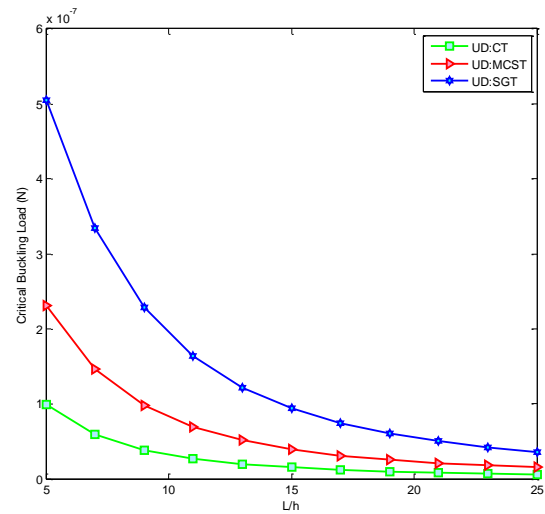
From Table 2, one can be observed that the results of present work are in good agreement with the obtained results by (Yas and Samadi 2012) for various boundary conditions.

The effect of aspect ratio ( $L/h$ ) on the value of non-dimensional natural frequency and critical buckling load for micro-composite USFG and UD beam with Simply-Simply (S-S) boundary conditions without considering longitudinal magnetic field is shown in Fig. 2. Moreover, comparison between the classical and non-classical beam models is depicted in this figure. Also, the results show that the dimensionless natural frequency and critical buckling load decrease with an increase in the aspect ratio. Also, among the various size-dependent effect, SGT and CT predict the highest and lowest values of non-dimensional fundamental frequency and critical buckling load for all values of  $L/h$ , respectively. So it reveals that the model based on SGT predicts the more value of stiffness among various types of size-dependent effect and this pattern is the same for all values of dimensionless three material length scale parameter. It is noted that with increasing of three material length scale parameter, the stiffness of tapered micro Reddy beam increases that this point leads to enhance the dimensionless natural frequency and critical buckling load and vice versa for aspect ratio.

The effect of aspect ratio ( $L/h$ ) and various distribution of CNT including UD, USFG and SFG on the dimensionless natural frequency and critical buckling load for S-S boundary conditions micro-composite beam based on SGT are shown in Figs. 3. According to these Figs., the dimensionless natural frequency and critical buckling load decreases for all types of distribution with increasing of the aspect ratio. Also it can be inferred that non-dimensional natural frequency and critical buckling load of FGX-CNTRC micro-composite beams are higher than those of beams with other CNTs distributions. The CNT distributions for SFG have most distant with respect to the neutral axis in comparison with other states such as USFG and UD-CNTRC, therefore, it is due to that its bending stiffness is larger than USFG and UD-CNTRC.

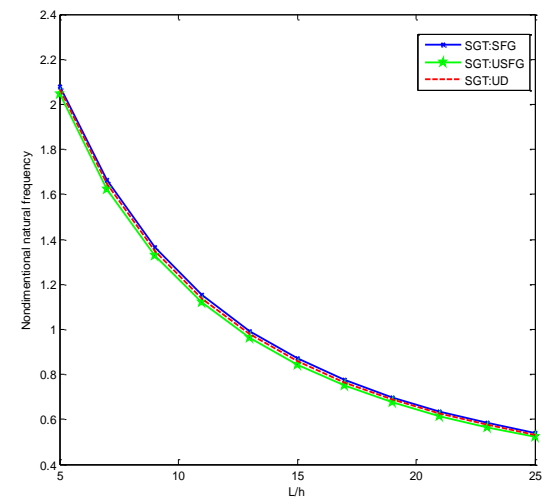


(a)



(b)

Fig. 2 The effect of various types of size-dependent effect on the (a) dimensionless natural frequency, (b) critical buckling for  $\alpha=1, \beta=0.5, H_x=0$  and  $l/h=1$



(a)

Fig. 3 The effect of various distribution of CNT on the (a) dimensionless natural frequency, (b) critical buckling load for  $\alpha=1, \beta=0.5, H_x=0$  and  $l/h=1$

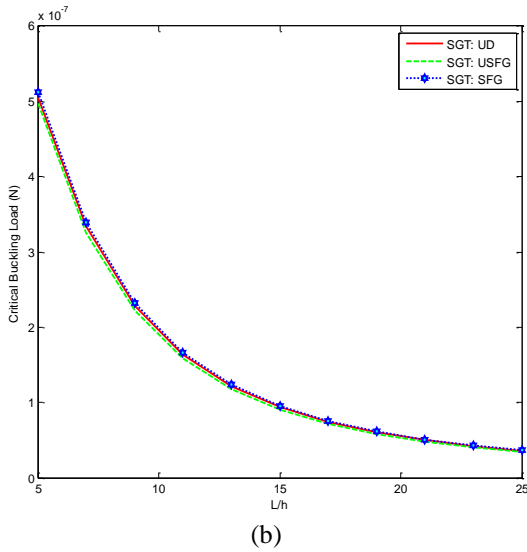
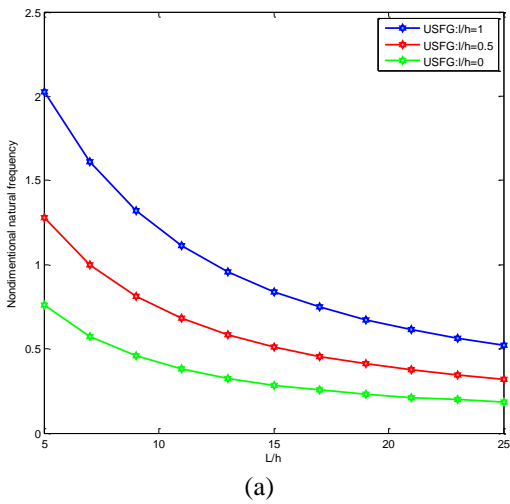
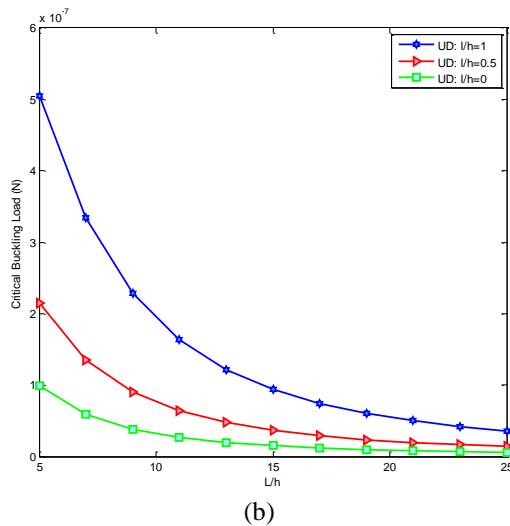


Fig. 3 Continued



(a)



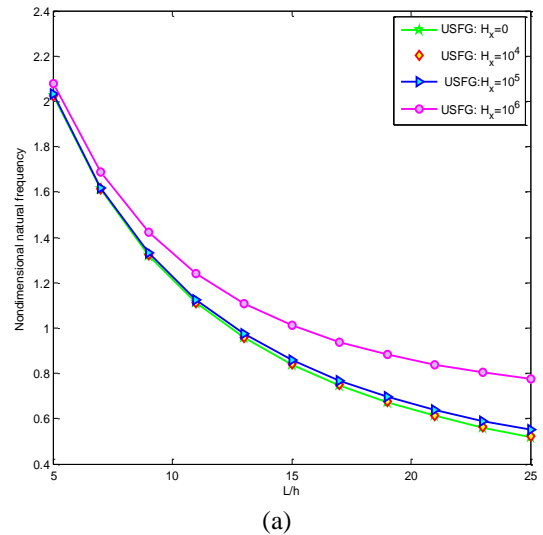
(b)

Fig. 4 Effect of length to thickness ratio ( $L/h$ ) on the (a) natural frequency and (b) critical buckling load of micro-composite beam for various  $l/h$ ,  $\alpha=1$ ,  $\beta=0.5$  and  $H_x=0$

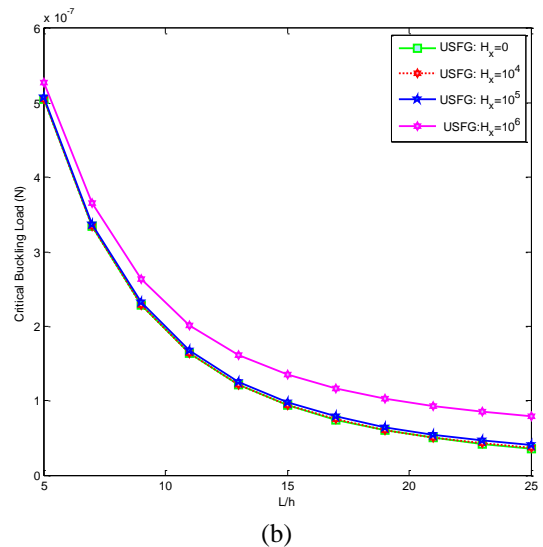
The influences of aspect ratio ( $L/h$ ) on the dimensionless

natural frequency and critical buckling load for different dimensionless material length scale parameters ( $l/h$ ) based on SGT are shown in Fig. 4, respectively. It is shown from the results that with increasing the dimensionless material length scale parameter, the non-dimensional natural frequency and critical buckling load increases for different aspect ratio ( $L/h$ ). Moreover, it is observed that the value of dimensionless length scale parameter plays more important role in the stiffness behaviour of FG-CNTRC micro-composite beam. On the other hands, employing the size dependent effect leads to enhance the stiffness of tapered micro Reddy beam and then increases the dimensionless natural frequency and critical buckling load.

Fig. 5 show the effects of magnetic fields on the non-dimensional natural frequency and critical buckling load. It can be observed that employing magnetic field in longitudinal direction of the micro-composite beam increases the natural frequency and critical buckling load while the longitudinal magnetic field has little influence on stiffer when its magnitude is small ( $<10^4$  A/m) over the



(a)



(b)

Fig. 5 Influence of the magnetic field  $H_x$  on the dimensionless natural frequency and critical buckling load for  $\alpha=1$ ,  $\beta=0.5$  and  $l/h=1$

entire frequency range. It means that the application of magnetic field leads to increase the SWCNT stiffer. So by increasing the imposed magnetic field significantly increases the stability of the system that can behave as an actuator. In this case, the stability of the system can be controlled by imposing magnetic field.

Fig. 6 show the effect of Winkler modulus on the non-dimensional natural frequency and critical buckling load of micro-composite USFG and UD beam based on SGT. The effect of Winkler foundation will appear in the stiffness matrix, therefore the non-dimensional natural frequency and critical buckling load will increase by increasing Winkler modulus for UD, USFG and SFG-CNTRC micro-composite beams. Also these changes in the non-dimensional natural frequency with the aspect ratio are found to be almost dependent on the change of the value of the Winkler modulus especially at higher values. At lower values of the elastic layer stiffness, this effect is found to be insignificantly dependent. It is stated that with an increase in the coefficient of elastic foundation, the stiffness of micro Reddy beam increases and then there is a direct relation between the stiffness of micro structures and non-dimensional natural frequency.

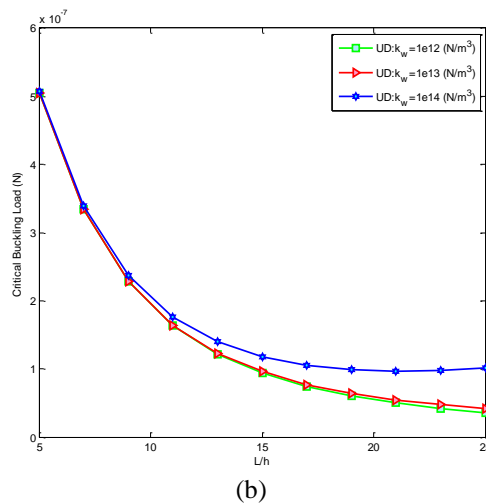
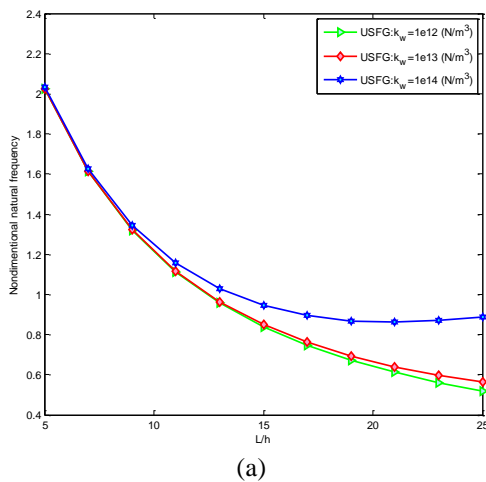


Fig. 6 Influence of the elastic parameter  $k_w$  on the dimensionless natural frequency and critical buckling load for  $\alpha=1$ ,  $\beta=0.5$ ,  $H_x=0$  and  $l/h=1$

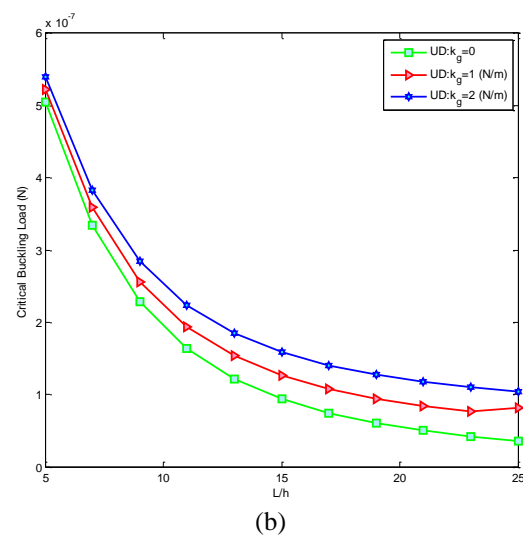
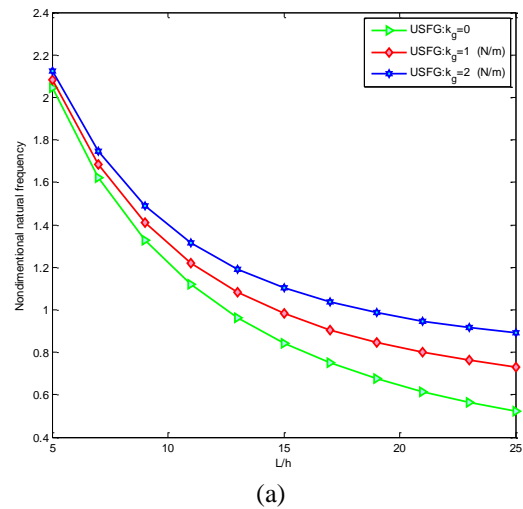
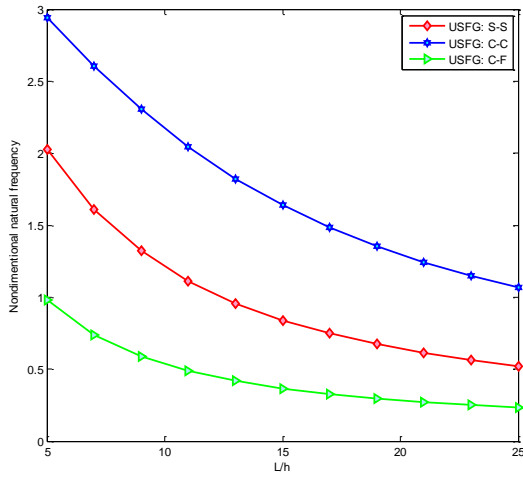


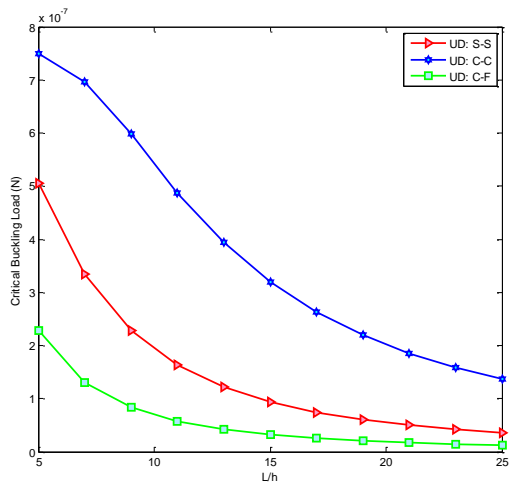
Fig. 7 Influence of the elastic parameter  $k_g$  on the dimensionless natural frequency and critical buckling load for  $\alpha=1$ ,  $\beta=0.5$ ,  $H_x=0$  and  $l/h=1$

Fig. 7 illustrate that the non-dimensional natural frequency and critical buckling load by SGT will increase by increasing Pasternak shear modulus. The effect of Pasternak foundation will appear in the stiffness matrix, therefore the natural frequency and critical buckling load will increase by increasing shear Pasternak modulus. It should be mentioned that the effects of  $k_g$  on the non-dimensional natural frequency and critical buckling load are more significant than those of  $k_w$ , and then the stability of system enhances.

Fig. 8 show the non-dimensional natural frequency and critical buckling load of C-C, S-S and C-F micro-composite UD and USFG beam for different aspect ratio. It can be seen that among the three boundary conditions considered, the C-F beam has the minimum values while the C-C beam has the maximum values of dimensionless natural frequency and critical buckling load. It is shown that the critical buckling load of FG-X CNTRC micro-composite beam is larger among these three types of beams. On the other hand, the FG-CNTRC micro beam becomes stiffer, then the stability of system enhances.

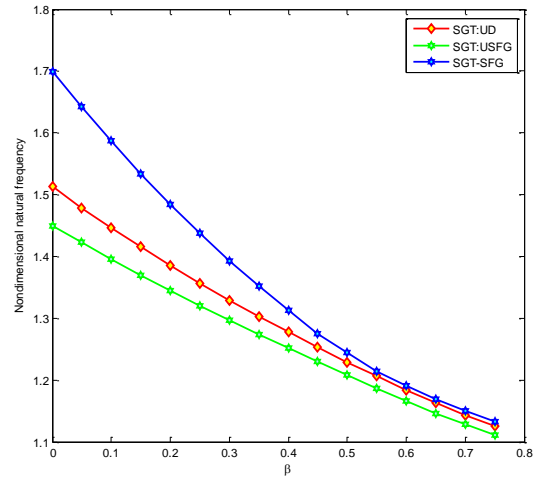


(a)

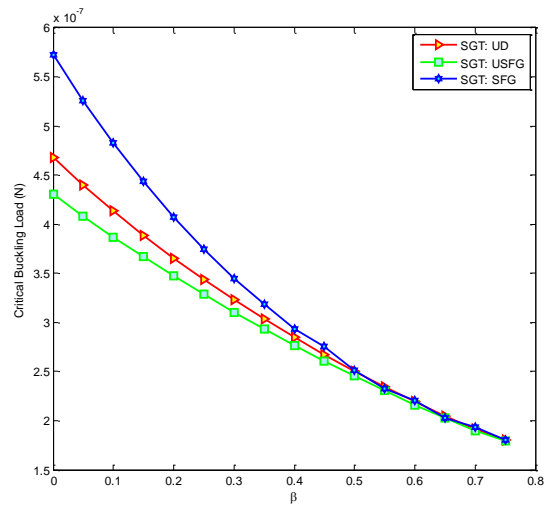


(b)

Fig. 8 The effect of various boundary conditions on the dimensionless natural frequency and critical buckling load of micro-composite beam for  $\alpha=1$ ,  $\beta=0.5$ ,  $H_x=0$  and  $l/h=1$



(a)

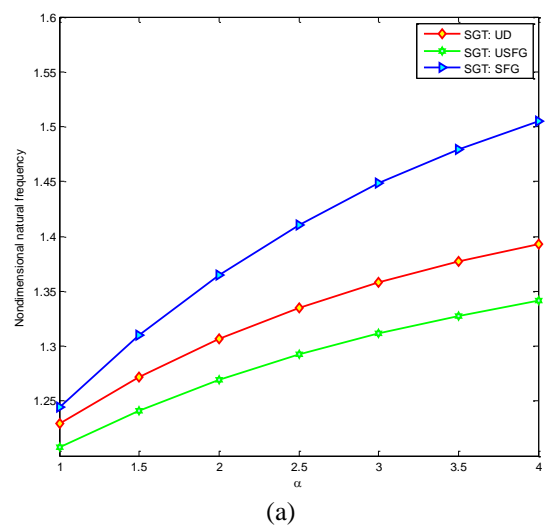


(b)

Fig. 9 The non-dimensional natural frequency and critical buckling load versus  $\beta$  for UD, USFG and SFG micro-composite beam

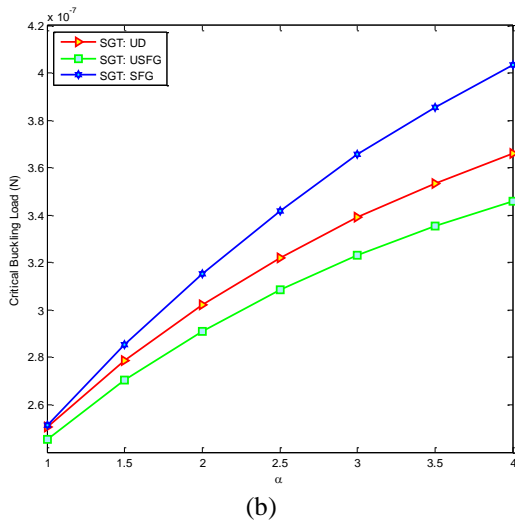
Fig. 9 indicate the non-dimensional natural frequency and critical buckling load versus variation value of  $\beta$  and  $\alpha=1$  for UD, USFG and SFG-CNTRC micro-composite beam. According to these Figs, increasing the tapered parameter leads to decrease the dimensionless natural frequency and critical buckling load for UD, USFG and SFG beam. Also at the specified value of  $\beta$ , the dimensionless natural frequency for SFG beam is more than for other state. It means that the USFG micro-composite beam causes to decrease the first natural frequency. Moreover, it is seen that for higher values of  $\beta$ , especially for  $\beta>0.5$ , the difference of non-dimensional natural frequency and critical buckling load between three cases decreases and it is not noticeable.

Fig. 10 show the non-dimensional natural frequency and critical buckling load versus variation value of  $\alpha$  and  $\beta=0.5$  for UD, USFG and SFG micro-composite beam. As it can be seen by an increase in  $\alpha$ , the non-dimensional natural frequency and critical buckling load increase but in the same value of  $\alpha$ , the value of natural frequency for SFG



(a)

Fig. 10 The non-dimensional natural frequency and critical buckling load versus  $\alpha$  for UD, USFG and SFG beam

(b)  
Fig. 10 Continued

beam is more than other state. Also, it is seen the frequencies of SFG-CNTRCs beam are higher than USFG and UD-CNTRC beams and this differences become larger with an increase in this parameter. Also, it is concluded that the effect of parameter  $\alpha$  on the non-dimensional natural frequency is less than the effect of tapered parameter  $\beta$ .

## 5. Conclusions

In this paper, the buckling and free vibration analysis of FG-CNTRC Reddy beam based on the strain gradient theory under longitudinal magnetic field using FEM is studied. In this research, the material property of matrix is considered as Poly methyl methacrylate (PMMA). Also, the effects of variation values of  $\beta$  and  $\alpha$ ; UD, USFG and SFG distributions of CNT on the critical buckling load and natural frequency are illustrated. Moreover, the influence of various boundary conditions on the dimensional natural frequency and critical buckling load is studied. The results of this research can be listed as follows:

1. With increasing  $\beta$ , the non-dimensional natural frequency and critical buckling load increase for UD, USFG and SFG beam and vice versa for  $\alpha$ . The parameter of  $\alpha$  has significant effect on the mode shapes of the micro-composite beams. Also it is concluded that the effect of non-uniformity parameter  $\alpha$  on the mode shapes is less than the effect of tapered parameter  $\beta$ .

2. For the tapered parameter  $\beta > 0.5$ , the FG-CNTRC distribution has insignificant effect on the non-dimensional frequency and critical buckling load and all micro-composite beams with different CNTs distributions are very close to each other.

3. At the specified value of  $\alpha$  and  $\beta$ , the dimensionless natural frequency and critical buckling load for SFG beam is more than the other state. The CNT distributions for SFG have most distant with respect to the neutral axis in comparison with other states such as USFG and UD-CNTRC, therefore, it is due to that its bending stiffness is larger than USFG and UD-CNTRC.

4. The effect of parameter  $\alpha$  on the non-dimensional natural frequency is less than the effect of tapered parameter  $\beta$ .

5. With an increase in Winkler modulus or Pasternak modulus is accompanied by increasing the non-dimensional natural frequency and critical buckling load. On the other hands, the employing the elastic foundation leads to enhance the stiffness of micro Reddy beam and then there is a direct relation between the stiffness of micro structures and non-dimensional natural frequency.

6. Reddy beam becomes stiffer with decreasing of aspect ratio.

7. The non-dimensional frequency and critical buckling load of micro-composite beam increases with an increase in the material length scale parameters. On the other hands, considering the size dependent effect leads to enhance the stiffness of tapered micro Reddy beam and then increases the dimensionless natural frequency and critical buckling load.

8. The non-dimensional natural frequency and critical buckling load of micro-composite beam increases with an increase in the magnetic field. Also, by increasing the imposed magnetic field significantly increases the stability of the system that can behave as an actuator. In this case, the stability of the system can be controlled by imposing magnetic field.

## Acknowledgments

The authors would like to thank the reviewers for their valuable comments. They are also grateful to the Iranian Nanotechnology Development Committee for their financial support and also grateful to the University of Kashan for supporting this work by Grant no. 463855/3.

## References

- Ansari, R., Faghih Shojaei, M., Gholami, Mohammadi, R., Mohammadi, V. and Darabi, M.A. (2013), "Thermal postbuckling behavior of size-dependent functionally graded Timoshenko micro-beams", *Int. J. Non-Linear Mech.*, **50**, 127-135.
- Chakraborty, A., Gopalakrishnan, S. and Reddy, J.N. (2003), "A new beam finite element for the analysis of functionally graded materials", *Int. J. Mech. Sci.*, **45**(3), 519-539.
- Chakraborty, A., Mahapatra, D.R. and Gopalakrishnan, S. (2002), "Investigated finite element analysis of free vibration and wave propagation in asymmetric composite beam with structural discontinuities", *Compos. Struct.*, **55**(1), 23-36.
- Ghiasian, S.E., Kiani, Y. and Eslami, M.R. (2014), "Non-linear rapid heating of FGM beams", *Int. J. Non-Linear Mech.*, **67**, 74-84.
- Ghorbanpour Arani, A., Atabakhshian, V., Loghman, A., Shajari, A.R. and Amir, S. (2012), "Nonlinear vibration of embedded SWBNNTs based on nonlocal Timoshenko beam theory using DQ method", *Physica. B.*, **407**(13), 2549-2555.
- Ghorbanpour Arani, A., Haghparast, E. and Zarei, H.B.A. (2016), "Vibration of axially moving 3-phase CNTFPC plate resting on orthotropic foundation", *Struct. Eng. Mech.*, **57**(1), 105-126.
- Ghorbanpour Arani, A., Amir, S., Shajari, A.R., Khoddami Maraghi, Z. and Mohammadimehr, M. (2012), "Electro-thermal

- non-local vibration analysis of embedded DWBNNTs”, *Proc. Ins. Mech. Eng., Part C: J. Mech. Eng. Sci.*, **226**(5), 1410-1422.
- Ghorbanpour Arani, A., Mobarakeh, M.R., Shams, S., Mohammadimehr, M. (2012), “The effect of CNT volume fraction on the magneto-thermo-electro-mechanical behavior of smart nanocomposite cylinder”, *J. Mech. Sci. Technol.*, **26**(8), 2565-2572.
- Giannopoulos, I.G. and Kallivokas, G. (2014), “Mechanical properties of graphene based nanocomposites incorporating a hybrid interphase”, *Finite Element Anal. Des.*, **90**, 31-40.
- Hemmatnezhad, M., Ansari, R. and Rahimi, G.H. (2013), “Large-amplitude free vibrations of functionally graded beams by means of a finite element formulation”, *Appl. Math. Model.*, **37**(18), 8495-8504.
- Heshmati, M. and Yas, M.H. (2013), “Vibrations of non-uniform functionally graded MWCNTs- polystyrene nano-composite beams under action of moving load”, *Mater. Des.*, **46**, 206-218.
- Heshmati, M. and Yas, M.H. (2013), “Dynamic analysis of functionally graded multi-walled carbon nanotube-polystyrene nano-composite beams subjected to multi-moving loads”, *Mater. Des.*, **49**, 894-904.
- Ishaquddin, M.D., Raveendranath, P. and Reddy, J.N. (2016), “Efficient coupled polynomial interpolation scheme for out-of-plane free vibration analysis of curved beams”, *Finite Element Anal. Des.*, **110**, 58-66.
- Kahrobaiyan, M.H., Asghari, M. and Ahmadian, M.T. (2014), “Strain gradient beam element”, *Adv. Compos. Mater.*, **68**, 63-75.
- Karimov, K.S., Abid, M., Saleem, M., Akhmedov, M., Bashir, M., Shafique, U. and Ali, M. (2014), “Temperature gradient sensor based on CNT composite”, *Physica B*, **446**, 39-42.
- Lam, D.C.C., Yang, F., Chong, A.C.M., Wang, J. and Tong, P. (2003), “Experiments and theory in strain gradient elasticity”, *J. Mech. Phys. Solid.*, **51**(8), 1477-1508.
- Lau, K.T., Gu, C., Gao, G.H., Ling, H.Y. and Reid, S. (2004), “Stretching process of single and multiwalled carbon nanotubes for nanocomposite”, *Appl. Carbon.*, **42**(2), 426-428.
- Mohammadimehr, M. and Rahmati, A.H. (2013), “Small scale effect on electro-thermo-mechanical vibration analysis of single-walled boron nitride nanorods under electric excitation”, *Turk J. Eng. Environ. Sci.*, **37**(1), 1-15.
- Mohammadimehr, M., Mohandes, M. and Moradi, M. (2016), “Size dependent effect on the buckling and vibration analysis of double-bonded nanocomposite piezoelectric plate reinforced by boron nitride nanotube based on modified couple stress theory”, *J.Vib. Control*, **22**(7), 1790-1807.
- Mohammadimehr, M., Rousta Navi, B. and Ghorbanpour Arani, A. (2015), “The free vibration of viscoelastic double-bonded polymeric nanocomposite plates reinforced by FG-SWCNTs using modified strain gradient theory (MSGT), sinusoidal shear deformation theory and meshless method”, *Compos. Struct.*, **131**, 654-671.
- Mohammadimehr, M., Monajemi, A.A. and Moradi, M. (2015), “Vibration analysis of viscoelastic tapered micro-rod based on strain gradient theory resting on visco-pasternak foundation using DQM”, *J. Mech. Sci. Technol.*, **29**(6), 2297-2305.
- Narendar, S., Gupta, S.S. and Gopalakrishnan, S. (2012), “Wave propagation in single-walled carbon nanotube under longitudinal magnetic field using nonlocal Euler-Bernoulli beam theory”, *Appl. Math. Model.*, **36**(9), 4529-4538.
- Rahmati, A.H. and Mohammadimehr, M. (2014), “Vibration analysis of non-uniform and non-homogeneous boron nitride nanorods embedded in an elastic medium under combined loadings using DQM”, *Physica. B.*, **440**, 88-98.
- Reddy, J.N. (2004), *An Introduction to nonlinear finite element analysis*, Oxford University Press, Oxford, New York, USA.
- Reddy, J.N. (1987), “Mixed finite element models for laminated composite plate”, *J. Eng. Indust.*, **109**, 39-45.
- Sahmani, S. and Ansari, R. (2013), “Size-dependent buckling analysis of functionally graded third-order shears deformable micro-beams including thermal environment effect”, *Appl. Math. Model.*, **37**(23), 9499-9515.
- Sahmani, S., Aghdam, M.M. and Bahrami, M. (2015), “On the free vibration characteristics of postbuckled third-order shear deformable FGM nano-beams including surface effects”, *Compos. Struct.*, **121**, 377-385.
- Shen, H. (2009), “Nonlinear bending of functionally graded carbon nanotube-reinforced composite plates in thermal environments”, *Compos. Struct.*, **91**(1), 9-19.
- Şimşek, M. (2014), “Nonlinear static and free vibration analysis of microbeams based on the nonlinear elastic foundation using modified couple stress theory and He’s variational method”, *Compos. Struct.*, **112**, 264-272.
- Taati, E., Molaei Najafabadi, M. and Reddy, J.N. (2014), “Size-dependent generalized thermo elasticity model for Timoshenko micro-beams based on strain gradient and non-Fourier heat conduction theories”, *Compos. Struct.*, **116**, 595-611.
- Yas, M.H. and Samadi, N. (2012), “Free vibrations and buckling analysis of carbon nanotube-reinforced composite Timoshenko beams on elastic foundation”, *Int. J. Press. Vessel. Pip.*, **98**, 119-128.
- Yas, M.H. and Heshmati, M. (2012), “Dynamic analysis of functionally graded nanocomposite beams reinforced by randomly oriented carbon nanotube under the action of moving load”, *Appl. Math. Model.*, **36**(4), 1371-1394.
- Zhang, B., He, Y., Liu, D., Gan, Z. and Shen, L. (2014), “Non-classical Timoshenko beam element based on the strain gradient elasticity theory”, *Finite Element Anal. Des.*, **79**, 22-39.
- Zhang, S., Yin, J., Zhang, H.W. and Chen, B.S. (2016), “A two-level method for static and dynamic analysis of multi-layered composite beam and plate”, *Finite Element Anal. Des.*, **11**, 1-18.

CC

